JACS
JOURNAL OF THE AMERICAN CHEMICAL SOCIETY
Article
pubs.acs.org/JACS

Exploring Key Orientations at Protein−Protein Interfaces with Small Molecule Probes

Eunhwa Ko,[†] Arjun Raghuraman,[†] Lisa M. Perez,[‡] Thomas R. Ioerger,*[,§] and Kevin Burgess*[,†]

[†]Department of Chemistry and [‡]Laboratory for Molecular Simulation, Texas A & M University, Box 30012, College Station, Texas 77842, United States

[§]Department of Computer Science, Texas A & M University, College Station, Texas 77843-3112, United States

Supporting Information

ABSTRACT: Small molecule probes that selectively perturb protein−protein interactions (PPIs) are pivotal to biomedical science, but their discovery is challenging. We hypothesized that conformational resemblance of semirigid scaffolds expressing amino acid side-chains to PPI-interface regions could guide this process. Consequently, a data mining algorithm was developed to sample huge numbers of PPIs to find ones that match preferred conformers of a selected semirigid scaffold. Conformations of one such chemotype (**1aaa**; all methyl side-chains) matched several biomedically significant PPIs, including the dimerization interface of HIV-1 protease. On the basis of these observations, four molecules **1** with side-chains corresponding to the matching HIV-1 dimerization interface regions were prepared; all four inhibited HIV-1 protease via perturbation of dimerization. These data indicate this approach may inspire design of small molecule interface probes to perturb PPIs.

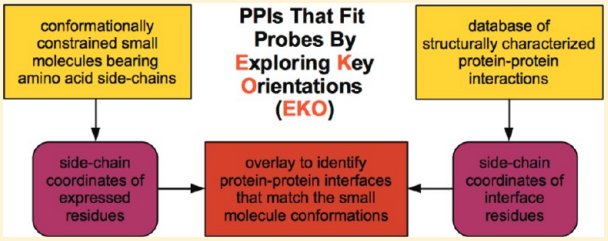

INTRODUCTION

Discovery of small molecules that perturb protein−protein interactions (PPIs) is often achieved by high-throughput screening (HTS), fragment- and structure-based strategies,[1−3] molecular evolution of macrocycles,[4] tethering,[2] target template click chemistry,[5] and design of secondary structure mimics.[6] However, the most prevalent method, HTS, gives disappointing hit rates relative to the cost and time expenditures involved, even if it is augmented by computational simulations based on matching virtual libraries with structural and physiochemical descriptors.[7,8]

Compound libraries for HTS assembled to find small molecules that bind enzyme active sites, ion channels, and G protein-coupled receptors, and filtered for predicted oral bioavailabilities,[9,10] may not be suitable for PPI targets; it has been suggested this is one reason for the poor hit rates.[11] Despite this, there is no widely accepted notion of preferred small molecule chemotypes for these targets, except for small molecule mimics of ideal interface secondary structures.[12,13] These *minimalist mimics* are comprised of nonpeptidic, semirigid skeletons that express amino acid side-chains, e.g., compound **1**[14] (Figure 1). This led us to hypothesize a set of privileged small molecule chemotypes for perturbation of PPIs and how they could be applied. Specifically, favorable conformations of semirigid small molecules expressing amino acid side-chains could be compared with PPI interfaces to find the PPI that best matches the molecule; we call this concept *Exploring Key Orientations* (EKO).

GUIDELINES FOR A SET OF SMALL MOLECULE CHEMOTYPES TO PERTURB PROTEIN−PROTEIN INTERACTIONS

Expression of amino acid side-chains on semirigid small molecules is a valuable concept because interactions between interface side-chains dominate PPIs;[15] however, in our view, secondary structure mimicry is not the overall end point because key interface regions are often formed from more than one, and/or from nonideal, secondary structure motifs. There are many PPI interface regions that cannot be mimicked by molecules that resemble *one ideal* secondary structure. Chemotypes for perturbing PPIs therefore should be based on comparing the orientations of the amino acid side-chains they project with those at protein−protein interfaces and not necessarily on secondary structure mimicry. Thus, the following *structural* design criteria were conceived for the chemotypes:

- synthetically accessible with any combination of at least three amino acid side-chains (e.g., Arg, Trp, His, etc.) to be incorporated onto a semirigid scaffold that has ...
- kinetically and thermodynamically accessible conformations (i.e., not too rigid) for induced fit to the protein binding partner but with ...
- only moderate loss of entropy on docking (i.e., the scaffold has only a few significant degrees of freedom that influence the side-chain orientations).

Received: July 13, 2012
Published: December 27, 2012

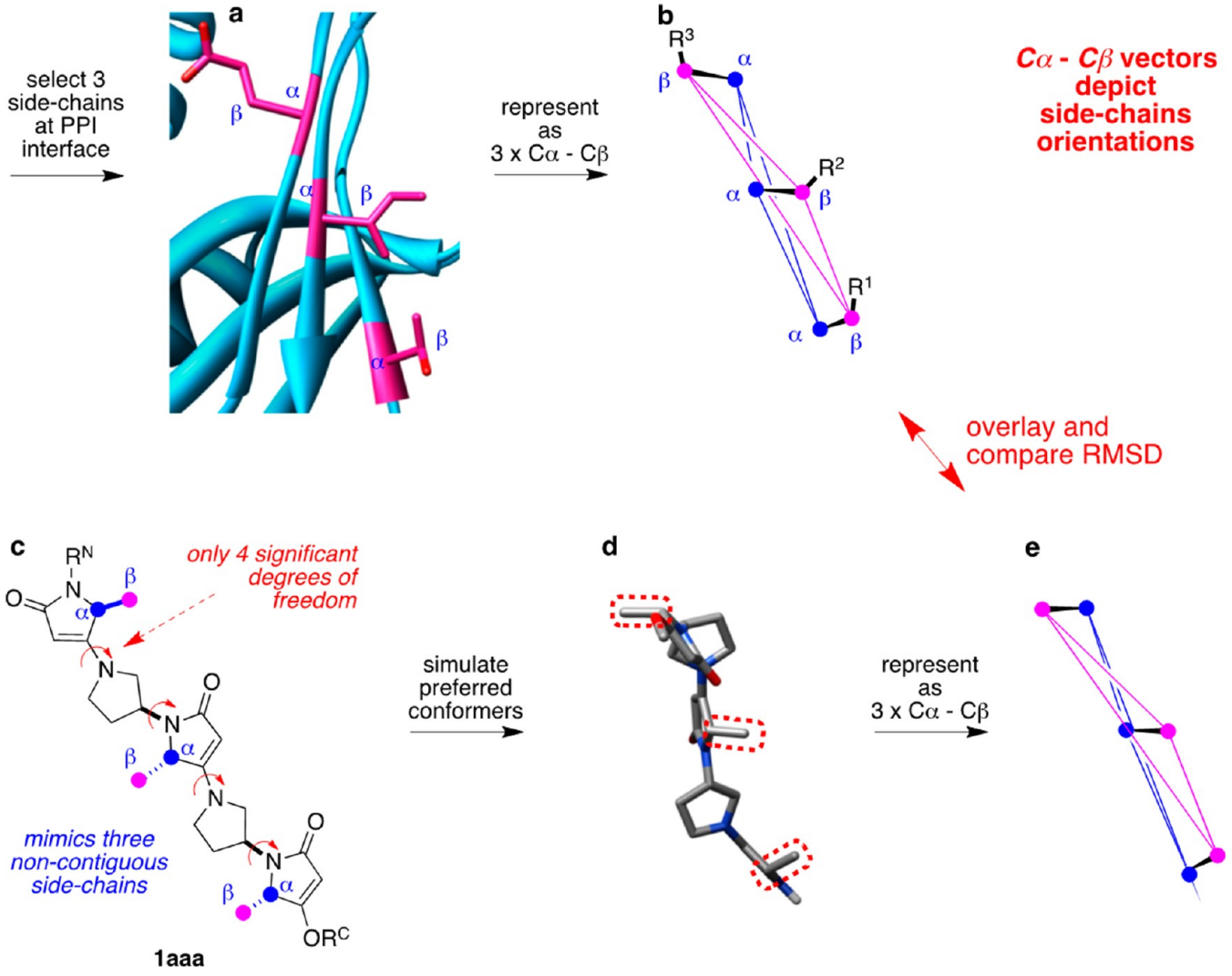

Figure 1. *Cα*−*Cβ* vectors depict how side-chains project at PPI interfaces (**a** and **b**) and in preferred conformations of semirigid small molecules that express amino acid side-chains (**c**−**e**). These side-chain orientations can be depicted as sets of six coordinates in three-dimensional space and overlaid; goodness of fit may be expressed using RMSD (root-mean-square values). The protein−protein interface shown is a region from heat-labile enterotoxin B_5 (PDB: 1eef).

Properties like water solubilities, toxicities, cell permeabilities, shelf lives, etc., are important, but different, issues. Justification for selection of three side-chains as a starting point for these guidelines is as follows. In our estimation, *two* side-chain analogues would tend to have inadequate affinities and selectivities. Combinations of *three* side-chains were chosen because tripeptides frequently display high affinities and selectivities in cell biology (reviewed,[16] e.g., RGD motifs). Four side-chain systems tend to be harder to prepare, and their allowed conformations probably would be too exclusive because this would involve matching eight coordinates (see below). The key parameters above are intended to be nonexclusive *structural* chemotype guidelines for identifying small molecules to perturb PPIs, and the EKO approach is specifically designed to work with these types of molecules.

■ DEVELOPMENT OF THE EKO APPROACH

Semirigid scaffolds presenting side-chains have multiple favorable core conformations. Implementation of EKO requires that side-chain orientations in these conformations be compared with projections of side-chains at protein−protein interfaces. If there is a good match in this comparison, then the small molecule might wholly or partially displace that protein from the PPI, thereby perturbing the interface. Complete dissociation at PPI interfaces is not essential because binding small molecules at PPIs may have biochemical ramifications even if they do not displace the protein binding partners[17] (cf. allosteric binding).

Computational methods are required to achieve the levels of insight required to compare side-chain orientations of a small molecule with those at PPI interfaces. Fortunately, once these methods have been worked out, this facilitates data mining on a massive scale, i.e., systematic and sequential sampling of many structurally characterized PPIs.

The first step in developing EKO was to establish bases for comparisons (Figure 1). Amino acid *Cα* and *Cβ* coordinates are the best simple defining characteristic of side-chain orientations since *Cβ*−*Cγ* vectors and atoms downstream of these are relatively mobile and do not define overall direction.[13] Preferred conformations of scaffolds that express only *Cα* and *Cβ* atoms, i.e., methyl-substituted ones, show how the molecular core tends to project *any* set of amino acid side-

dx.doi.org/10.1021/ja3067258 | J. Am. Chem. Soc. 2013, 135, 167−173

chains. For example, favorable conformations of the Ala-Ala-Ala derivative **1aaa** in medium with a continuous dielectric of 80 can be reduced to a set of six coordinates (3(*Cα* + *Cβ*)) that represent the scaffold bias when unperturbed by side-chain functionalities or explicit water molecule effects.

Orientations of side-chains in PPIs can be represented by *Cα* and *Cβ* coordinates from crystallographic data. Only side-chains that are physically able to interact with the protein binding partner need be considered, hence filters were devised. Thus only side-chains within *X* Å of a chain on the other protein are selected, where "*X*" is a user-defined parameter (set at 4 Å in this work). An interface residue is defined as a residue for which "any side-chain atom" of a protein comes within *X* Å of "any" non-*H* atom in the partner protein. For instance, the atoms C*β*, C*γ*1, and C*γ*2 of Val would be considered, as would the terminal −*OH* and C*β* of Tyr.

To implement EKO (Figure 2), preferred conformations of a semirigid small molecule with methyl side-chains must first be

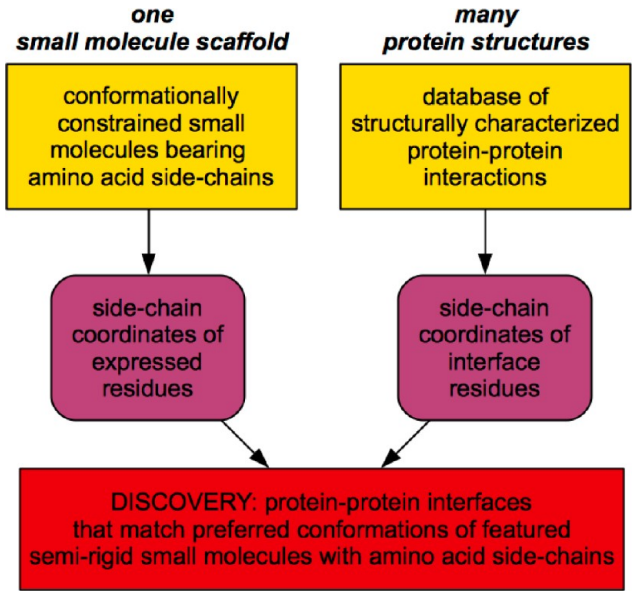

Figure 2. Preferred conformers of small molecules are determined and the side-chain *Cα* and *Cβ* coordinates for each are recorded. The algorithm determines the interface residues of each PPI in a database and sequentially matches each combination of three interface side-chains with the three side-chains of the small molecule and outputs goodness of fit for every overlay as RMSDs.

simulated; here quenched molecular dynamics (QMD)[13,18] was used to do this, and only conformers within 3 kcal/mol of the most stable one identified were considered. This "3 kcal/mol cut-off" gave the following number of conformers for each stereoisomer of **1**: LLL- (490), DLL- (490), LDL- (453), LLD- (512), LDD- (489), DLD- (511), DDL- (487), and DDD- (466). To save CPU, the analysis does not use all those conformations; instead, they are clustered into families with similar RMSDs based on C*α* and C*β* coordinates, and poorly represented conformers from each family are removed (ca. 20−30% of the QMD conformers; see Table S1 and the surrounding discussion in the Supporting Information for the exact numbers and procedure).

The data mining algorithm developed here takes each preferred conformation as an input, expresses it as six coordinates {3(*Cα* + *Cβ*)}, and quantifies the "goodness of fit" of these on all combinations of three amino acid side-chains in all the structurally characterized PPI interfaces that are entered. Using the Texas A & M supercomputing facility, over 53,000 PPI interfaces corresponding to 15,736 structures were sampled in less than 6 h per **1aaa** stereoisomer. For eight stereomers of **1aaa**, EKO exposed a total of 391 unique PPI-interface regions where orientations of side-chains in preferred conformations matched those at interfaces with RMSDs ≤0.30 Å (Table S2, Supporting Information).

The output of this algorithm (Tables S3−S10, Supporting Information) is a relatively long list of interface regions that matched with preferred conformers of the featured compound. Data from mining a single isomer of **1** take too much space to show here, but Table 1 illustrates an EKO output for the 11

Table 1. Summary for Stereomer L,L,L-1aaa from EKO

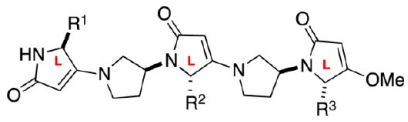

L,L,L-1aaa

entry	PDB	protein homo- or hetero-oligomer	RMSD (Å)	residues (R^1−R^2−R^3)
1	1kn0	Rad52	0.14	H121−S119−D117
2	1n2c	nitrogenase	0.19	K145−D76−S257
3	1g0o	trihydoxynaphthalene reductase	0.23	P173−H122−V126
4	1j3u	aspartase	0.23	V236−T234−V232
5	1gl7	TrwB	0.23	T352−D349−S346
6	1six	trypsin-ecotin	0.24	Me5−T83−L52
7	3pcb	3,4-PCD[a]	0.24	Q177−175−K173
8	1fcj	*O*-acetylserine sulfhydrylase	0.24	L268−S301−E303
9	2f4f	IS200 transposase	0.25	H60−V18−V107
10	1mtp	serpin (thermopin)	0.26	Y200−T210−A218
11	1eef	heat-labile enterotoxin	0.26	T47−I39−E29
15	1thz	AICAR Tfase[b]	0.28	A218−L220−T222
16	3gpd	GAPDH[c]	0.28	T228−M230−F232
23	1hpv	HIV-1 protease	0.29	L97−C95−I93

[a]3,4-PCD: protococatechuate 3,4-dioxygenase. [b]AICAR Tfase: avian aminoimidazole-4-carboxamide ribonucleotide transformylase. [c]GAPDH: D-glyceraldehyde 3-phosphate dehydrogenase.

best "hit" interface overlays, and three others, from L,L,L-**1aaa**. Entries 15, 16, and 23 are, in our view, biomedically significant PPI targets that would interest researchers considering synthesis of molecules with type **1** chemotypes.

In the procedure above, preferred conformations of the featured scaffold are calculated using truncated (Me-) side-chains, but they are overlaid on *Cα* and *Cβ* coordinates corresponding to combinations of *particular* interface amino acids. By making this comparison, EKO searches for intrinsic conformational biases of the scaffold with methyl side-chains that will be *reinforced* when the molecule binds a protein-binding partner in a hit PPI. Synergy occurs in these situations because the favored scaffold *Cα*−*Cβ* orientations coincide with the ways the rest of these side-chains are bound by the protein binding partner at the PPI interface.

EKO side-steps the most problematic issues encountered in simulations of small molecules interacting with protein surfaces by focusing on static interface regions in structurally characterized PPIs. Structural data clearly show the interface regions and the side-chain orientations circumventing the issue

dx.doi.org/10.1021/ja3067258 | J. Am. Chem. Soc. 2013, 135, 167−173

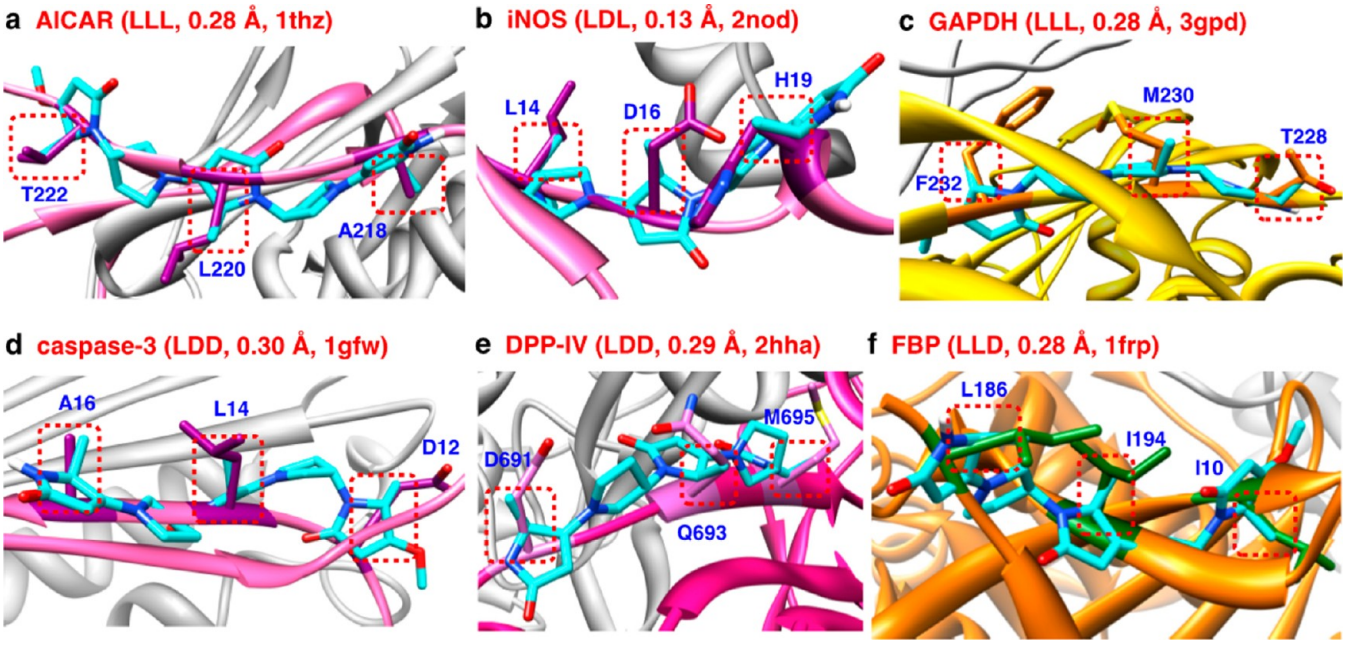

Figure 3. Selected PPIs that match preferred conformations of **1aaa**. (**a**) 5-Aminoimidazole-4-carboxamide ribonucleotide transformylase (AICAR Tfase: an enzyme in purine biosynthesis. Cancer cells depend on *de novo* purine biosynthesis, hence they are vulnerable to AICAR Tfase inhibitors).[19] (**b**) Inducible Nitric Oxide Synthase (iNOS; implicated in inflammatory, autoimmune diseases, and cancers).[20] (**c**) D-GlycerAldehyde-3-Phosphate DeHydrogenase (GAPDH; implicated in neurodegenerative apoptotic cell death).[21] (**d**) Caspase 3 (pivotal in apoptotic neural cell death in Parkinson's,[22] ALS,[23] Huntington's, and Alzheimer's diseases).[24] (**e**) DiPeptidyl Peptidase (DDP-4; a serine protease target for treatment of type 2 diabetes).[25] (**f**) Fructose-1,6-BisPhosphatase (FBP; modulates gluconeogenesis and is another target for controlling type 2 diabetes).[26]

of how the small molecule and protein might flex to adapt to each other. EKO determines situations where the structurally characterized PPI and favored conformations of the small molecule have similar side-chain orientations: if there are no anomalies in the structural data, then those side-chains are sterically and physiochemically matched.

In unpublished work (in preparation), we have simulated all accessible conformers of eight well-known putative α-helical minimalist mimics and compared their side-chain orientations with those for ideal α-helical structures. None of the conformers of these compounds matched ideal α-helical structures with an RMSD of less than 0.30 Å. On the basis of this study, and other unpublished work, we suggest RMSD <0.30 Å is a stringent test for matching three side-chains in interface mimics.

Mining the eight stereoisomers of **1aaa** on over 53,000 structurally characterized PPIs gave *only two* instances with RMSDs ≤0.30 Å in which the same three side-chains were implicated for different PPI targets. This observation suggests good selectivity is possible, probably via two origins. First, if L- and D-isomers of the protein encoded amino acids can be used at every position, then one particular combination is a 1 in 59,319 occurrence. Exactly the same reasoning would apply for tripeptides, but the second origin of selectivity, an entropy parameter, is more applicable to semirigid small molecules. Semirigid chemotypes access far fewer conformations than similar peptides, so they are statistically less likely to match at a PPI interface, hence the exclusivity of any hit found is higher.

Figure 3 shows six PPIs selected from the 391 that EKO found to match preferred conformers of **1aaa**. Brief descriptions of each are given in the figure caption to illustrate why they are high-interest targets for medicinal chemistry. This set of only six targets contains ones that impact cancer, neurodegenerative diseases, and type 2 diabetes.

As far as we are aware, there is no precedent for the EKO approach. For instance, CAVEAT[27−30] is operationally distinct and has different objectives. CAVEAT searches for molecular frameworks that can position functional groups in specific relative orientations in enzyme active sites by screening *multiple ligands for a specified protein cavity*, almost invariably to find enzyme inhibitors, and it does *not* use a protein-binding partner to guide the selection of the ligands. Conversely, EKO uses one protein in a PPI as a template to identify small molecules that may bind the other protein; there is no parallel for this in CAVEAT. There is also nothing in CAVEAT to sequentially address different regions in PPI interfaces. The main similarity connecting CAVEAT and EKO is that they both involve data mining: CAVEAT mines different small molecules for fit cavities in proteins selected by the user, while EKO searches different PPIs given a user-defined starting molecule.

■ VALIDATION OF EKO USING HIV-1 PROTEASE

We looked for one test case to validate the EKO method experimentally. EKO revealed preferred conformations of **1aaa** overlaid on two "side-chain triplets" on the HIV-1 protease dimerization region: Leu97-Cys95-Ile93 (RMSD 0.29 Å; Figure 4) and Phe99-Leu97-Cys95 (0.33 Å). This dimer interface has hot spots[11] at Cys95-Thr96-Leu97-Asn98-Phe99.[31] Mutation of Cys95 to Ala has little impact on the protease activity[32] and presumably on the dimerization energy too, so **1la**i-H and **1fla**-H were prepared[14] where methyl side-chains substitute for CH_2SH, making the synthesis significantly more convenient.

Inhibition of HIV-1 protease was measured via a fluorescence-based assay,[33] and then Zhang−Poorman kinetic analyses[34] were performed to determine if the inhibitors disrupt the dimer interface. Several intermediates in the syntheses of compounds **1** that have only two amino acid side-chains on the scaffold were tested, i.e., compounds **2**. One of these (**2la**-H)

dx.doi.org/10.1021/ja3067258 | J. Am. Chem. Soc. 2013, 135, 167−173

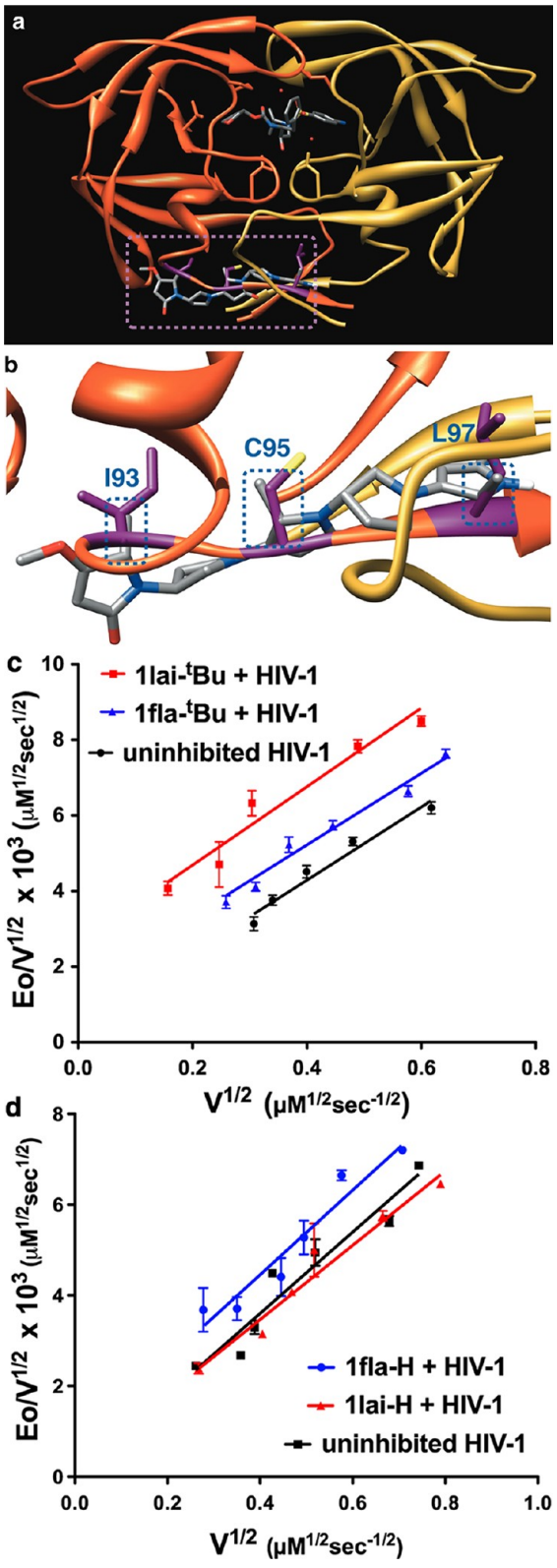

Figure 4. Disruption of the HIV-1 protease dimer. (**a**) Structure of HIV-1 protease (1hpv) showing the relevant dimer interface region box that was exposed by EKO. (**b**) Original overlay identified on *C*-terminal ICL of the protease (RMSD 0.29 Å). Zhang–Poorman analyses of (**c**) **1lai**-^{t}Bu (100 μM), **1fla**-^{t}Bu (50 μM), and uninhibited HIV-1 (i.e., substrate only, no inhibitor) and (**d**) **1lai**-H (5 μM), **1fla**-H (50 μM), and uninhibited HIV-1. *V* = initial velocity, and Eo = total enzyme concentration. Based on at least three runs for each data point.

gave no measurable inhibition of the protease, while another four gave IC_{50} values in the high micromolar range (**2la**-^{t}Bu, 176.4 μM; **2li**-H, 623.2 μM; **2fl**-^{t}Bu, 516.3 μM; **2fl**-H, 418.7 μM; Table S11, Supporting Information). These data support the assertion made above that semirigid scaffolds bearing only two amino acid side-chains tend to give relatively poor binding affinities.

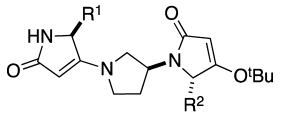

2

All four of the featured compounds **1** inhibited HIV-1 protease more effectively than the two side-chain intermediates **2** (Figure 4; **1lai**-H: IC_{50} = 3.7 ± 0.3 μM, K_i = 0.38 ± 0.07 μM; **1fla**-H: IC_{50} = 46.5 ± 8.0 μM, K_i = 0.93 ± 0.2 μM; **1lai**-^{t}Bu: IC_{50} = 111.1 ± 18 μM, K_i = 19.4 ± 4.1 μM; **1fla**-^{t}Bu, IC_{50} = 54.9 ± 5.7 μM, K_i = 21.0 ± 2.1 μM). Zhang–Poorman analyses indicated that all four compounds acted via dimerization disruption. The K_i of the best hit, **1lai**-H, is comparable with optimized HIV-1 dimerization inhibitors reported in the literature (Figure S13, Supporting Information).[34−42] Known HIV-1 protease dimerization inhibitors tend to be long peptide sequences corresponding to *two* regions in the dimeric interface (Figure S13, Supporting Information). Conversely, the assayed compounds **1** are *nonpeptidic* small molecules with sequences corresponding to *one* set of three amino acids.

Inhibition by compounds that perturb HIV-1 protease dimerization tends to be inversely dependent on enzyme concentration.[34,39] One compound, **1fla**-^{t}Bu, was tested, and the inhibition of HIV-1 protease indeed decreased by a factor of 8 when a 5× higher HIV-1 protease dimer concentration was used (Supporting Information, Table S12). However, a similar inverse dependence on enzyme concentration also would be expected if the compounds formed aggregates that inhibited nonselectivity.[43−45] This was a valid concern because the featured compounds contain hydrophobic side-chains (corresponding to alanine, isoleucine, leucine, and phenylalanine). Consequently, the possible aggregation issue was addressed by comparing inhibition in the presence and absence of 0.1% Triton X-100 (Table 2).[43−45] Within experimental error, the initial velocities for a given compound do not change with and without Triton X-100, indicating the molecules are *not* promiscuous inhibitors acting through aggregation.

Table 2. Comparison of Initial Velocities with and Without 0.1% Triton X-100[a]

entry	compounds	normalized initial velocities[b] with 0.1% Triton X-100 (fluorescence units/s)	initial velocities Without 0.1% Triton X-100 (fluorescence units/s)
1	**1lai**-^{t}Bu	5.84 ± 0.78	5.48 ± 0.46
2	**1lai**-H	5.28 ± 0.90	5.29 ± 0.49
3	**1fla**-^{t}Bu	3.42 ± 1.22	3.74 ± 0.69
4	**1fla**-H	2.21 ± 0.40	2.06 ± 0.31

[a]In buffer of 0.1 M sodium acetate, 1.0 M sodium chloride, 1.0 mM EDTA, 1.0 mM DTT, 10% DMSO, and 1.0 mg/mL of BSA, pH 4.7. [b]Control experiments showed that Triton X-100 at 0.1% (by volume) altered the initial velocities for cleavage of the fluorogenic substrate in the *absence* of compounds **1**; consequently, a factor reflecting this perturbation was applied to give the normalized velocities indicated. Consequently, data in columns 3 and 4 can be compared, but relative rates for entries 1−4 cannot.

dx.doi.org/10.1021/ja3067258 | *J. Am. Chem. Soc.* 2013, 135, 167−173

Verification that the featured compounds **1** acted as dimerization inhibitors was not conveniently possible via analytical gel ultracentrifugation since molecules **1** and HIV-1 protease have similar UV absorption profiles (e.g., at 280 nm; see Supporting Information) complicating detection. Consequently, qualitative cross-linking experiments analyzed by gel electrophoresis were undertaken instead.[46] Figure 5 is an

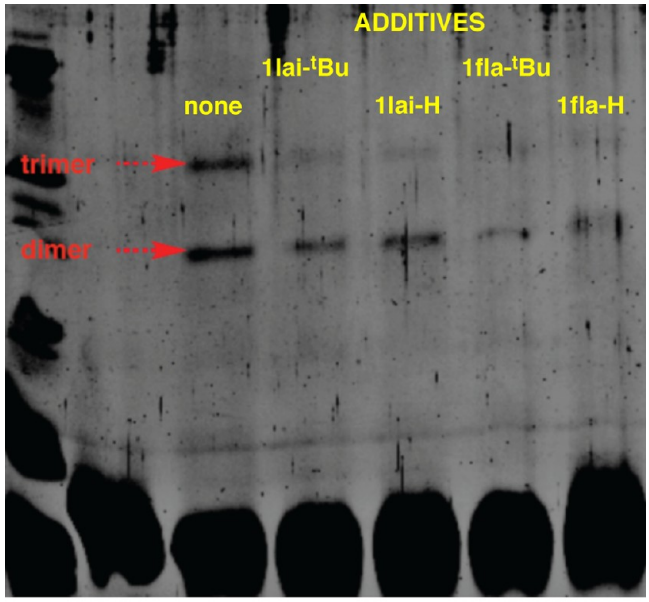

Figure 5. Formation of cross-linked HIV-1 protease dimer is suppressed by all four featured compounds **1**. This experiment was duplicated (see Supporting Information).

imaged gel showing the result of incubating the test compounds (200 μM) with the protease (10 μM) for 2 h at room temperature and then with a cross-linking agent (BS3) for 20 min at 37 °C. Quantitation was not attempted because of overlapping bands in the gels, possibly due to unfolding and autoproteolysis of the enzyme under these conditions; nevertheless, the result is clear: all four of the test compounds suppressed the amount of cross-linked dimer formed under these conditions.

CONCLUSION

A major limitation to the design of minimalist secondary structure mimics has been to generate structures that are selective for specific PPIs. A key innovation described here is to address that issue by using data mining for the *reverse* process: to find PPIs that match preferred small molecule conformations of the featured interface mimic. Moreover, the EKO approach can be applied irrespective of whether the small molecule resembles a secondary structure or not. It is the inverse of HTS where an assay is selected for a particular PPI and huge libraries are screened against it; consequently, EKO is *chemistry-driven*, whereas HTS and the other approaches currently used *focus on the protein target selected*. As far as we are aware, EKO is the first data mining approach to match PPIs with probes via virtual affinity selection from a huge PPI library using specific small molecule baits.

Researchers who are currently focused on one particular PPI may apply the EKO approach to single specific structurally characterized PPI targets; the chances of finding a good match are less than if it is coupled with data mining, but this approach can be rewarding (unpublished data). We believe the EKO method may lead chemists to identify PPIs that are most likely to be perturbed by molecules they have designed, and managers who oversee early stage drug discovery may decide to devote a fraction of their HTS budget to explore the cost effectiveness of EKO for PPI targets. We are currently exploring the feasibility of performing the EKO process using a powerful desktop personal computer to avoid the need for expensive computing equipment, and the initial indications are that this is viable. Further developments of this kind should significantly expand the user-base for this compound. At a minimum, it is an idea-generation method to inspire the design of small molecule interface probes to perturb PPIs.

ASSOCIATED CONTENT

Supporting Information

Development of the algorithm; figures, tables, and discussion to accompany the data mining experiments; procedures for HIV-1 protease inhibition and the Zhang–Poorman assays; literature on HIV-1 protease dimerization inhibitors; structures of all compounds tested; comparison of initial velocities in HIV-1 protease inhibition with and without Triton X-100; UV spectrum of **1fla**; procedures for enzyme cross-linking experiments. This material is available free of charge via the Internet at http://pubs.acs.org.

AUTHOR INFORMATION

Corresponding Author

burgess@tamu.edu

Notes

The authors declare no competing financial interest.

ACKNOWLEDGMENTS

We thank Mr. Dongyue Xin for performing the tests for aggregation via enzyme kinetics experiments and gratefully acknowledge Dr. Larry Dangott and the Texas A&M University Protein Chemistry Laboratory for help with the cross-linking experiments. HIV-1 protease (Q7K) was kindly provided by Dr. Celia Schiffer at University of Massachusetts Medical School. The National Institutes of Health (GM087981) and The Robert A. Welch Foundation (A-1121) provided financial support, and the Texas A&M Supercomputing Facility (http://sc.tamu.edu/) provided computing resources for the research reported in this paper.

REFERENCES

(1) Rees, D. C.; Congreve, M.; Murray, C. W.; Carr, R. *Nature* **2004**, *3*, 660–672.
(2) Erlanson, D. A.; Braisted, A. C.; Raphael, D. R.; Randal, M.; Stroud, R. M.; Gordon, E. M.; Wells, J. A. *Proc. Natl. Acad. Sci. U.S.A.* **2000**, *97*, 9367–9372.
(3) Zinzalla, G.; Thurston, D. E. *Future Med. Chem.* **2009**, *1*, 65–93.
(4) Gartner, Z. J.; Tse, B. N.; Grubina, R.; Doyon, J. B.; Snyder, T. M.; Liu, D. R. *Science* **2004**, *305*, 1601–1605.
(5) Kulkarni, S. S.; Hu, X.; Doi, K.; Wang, H.-G.; Manetsch, R. *ACS Chem. Biol.* **2011**, *6*, 724–732.
(6) Perez de Vega, M. J.; Martin-Martinez, M.; Genzalez-Muniz, R. *Curr. Top. Med. Chem.* **2007**, *7*, 33–62.
(7) Sperandio, O.; Miteva, M. A.; Villoutreix, B. O. *Methods Princ. Med. Chem.* **2011**, *48*, 435–465.
(8) Meireles, L. M. C.; Mustata, G. *Curr. Top. Med. Chem. (Sharjah, United Arab Emirates)* **2011**, *11*, 248–257.
(9) Lipinski, C. A.; Lombardo, F.; Dominy, B. W.; Feeney, P. J. *Adv. Drug Delivery Rev.* **1997**, *23*, 3–25.

(10) Miller, J. L. *Curr. Top. Med. Chem.* **2006**, *6*, 19−29.
(11) Wells, J. A.; McClendon, C. L. *Nature* **2007**, *450*, 1001−1009.
(12) Ko, E.; Liu, J.; Burgess, K. *Chem. Soc. Rev.* **2011**, *40*, 4411−4421.
(13) Ko, E.; Ling, J.; Perez, L. M.; Lu, G.; Schaefer, A.; Burgess, K. *J. Am. Chem. Soc.* **2011**, *133*, 462−477.
(14) Raghuraman, A.; Ko, E.; Perez, L. M.; Ioerger, T. R.; Burgess, K. *J. Am. Chem. Soc.* **2011**, *133*, 12350−12353.
(15) Conte, L. L.; Chothia, C.; Janin, J. *J. Mol. Biol.* **1999**, *285*, 2177−2198.
(16) Ung, P.; Winkler, D. A. *J. Med. Chem.* **2011**, *54*, 1111−1125.
(17) Thiel, P.; Kaiser, M.; Ottmann, C. *Angew. Chem., Int. Ed.* **2012**, *51*, 2012−2018.
(18) O'Connor, S. D.; Smith, P. E.; Al-Obeidi, F.; Pettitt, B. M. *J. Med. Chem.* **1992**, *35*, 2870−2881.
(19) Greasley, S. E.; Horton, P.; Ramcharan, J.; Beardsley, G. P.; Benkovic, S. J.; Wilson, I. A. *Nat. Struct. Biol.* **2001**, *8*, 402−406.
(20) Floyd, R. A.; Kotake, Y.; Towner, R. A.; Guo, W.-X.; Nakae, D.; Konishi, Y. *J. Toxicol. Pathol.* **2007**, *20*, 77−92.
(21) Chuang, D.-M.; Hough, C.; Senatorov, V. V. *Annu. Rev. Pharmacol. Toxicol.* **2005**, *45*, 269−290.
(22) Hartmann, A.; Hunot, S.; Michel, P. P.; Muriel, M.-P.; Vyas, S.; Faucheux, B. A.; Mouatt-Prigent, A.; Turmel, H.; Srinivasan, A.; Ruberg, M.; Evan, G. I.; Agid, Y.; Hirsch, E. C. *Proc. Natl. Acad. Sci.* **2000**, *97*, 2875−2880.
(23) Pasinelli, P.; Houseweart, M. K.; Brown, R. H., Jr.; Cleveland, D. W. *Proc. Natl. Acad. Sci.* **2000**, *97*, 13901−13906.
(24) D'Amelio, M.; Cavallucci, V.; Cecconi, F. *Cell Death Differ.* **2010**, *17*, 1104−1114.
(25) Herman, G. A.; Stein, P. P.; Thornberry, N. A.; Wagner, J. A. *Clin. Pharmacol. Ther.* **2007**, *81*, 761−767.
(26) Poelji, P. D.; Dang, Q.; Erion, M. D. *Drug Discovery Today: Ther. Stategies* **2007**, *4*, 103−109.
(27) Lauri, G.; Bartlett, P. A. *J. Comput.-Aided Mol. Des.* **1994**, *8*, 51−66.
(28) Sefler, A. M.; Lauri, G.; Bartlett, P. A. *Int. J. Pept. Protein Res.* **1996**, *48*, 129−138.
(29) Etzkorn, F. A.; Guo, T.; Lipton, M. A.; Goldberg, S. D.; Bartlett, P. A. *J. Am. Chem. Soc.* **1994**, *116*, 10412−10425.
(30) Yang, Y.; Nesterenko, D. V.; Trump, R. P.; Yamaguchi, K.; Bartlett, P. A.; Drueckhammer, D. G. *J. Chem. Inf. Model.* **2005**, *45*, 1820−1823.
(31) Todd, M. J.; Semo, N.; Freire, E. *J. Mol. Biol.* **1998**, *283*, 475−488.
(32) Davis, D. A.; Dorsey, K.; Wingfield, P. T.; Stahl, S. J.; Kaufman, J.; Fales, H. M.; Levine, R. L. *Biochemistry* **1996**, *35*, 2482−2488.
(33) Matayoshi, E. D.; Wang, G. T.; Krafft, G. A.; Erickson, J. *Science* **1990**, *247*, 954.
(34) Zhang, Z. Y.; Poorman, R. A.; Maggiora, L. L.; Heinrikson, R. L.; Kezdy, F. J. *J. Biol. Chem.* **1991**, *266*, 15591−15594.
(35) Lee, S.-G.; Chmielewski, J. *ChemBioChem* **2010**, *11*, 1513−1516.
(36) Shultz, M. D.; Bowman, M. J.; Ham, Y.-W.; Zhao, X.; Tora, G.; Chmielewski, J. *Angew. Chem., Int. Ed.* **2000**, *39*, 2710−2713.
(37) Bowman, M. J.; Chmielewski, J. *Bioorg. Med. Chem.* **2009**, *17*, 967−976.
(38) Bannwarth, L.; Rose, T.; Dufau, L.; Vanderesse, R.; Dumond, J.; Jamart-Gregoire, B.; Pannecouque, C.; De Clercq, E.; Reboud-Ravaux, M. *Biochemistry* **2009**, *48*, 379−387.
(39) Davis, D. A.; Brown, C. A.; Singer, K. E.; Wang, V.; Kaufman, J.; Stahl, S. J.; Wingfield, P.; Maeda, K.; Harada, S.; Yoshimura, K.; Kosalaraksa, P.; Mitsuya, H.; Yarchoan, R. *Antiviral Res.* **2006**, *72*, 89−99.
(40) Vidu, A.; Dufau, L.; Bannwarth, L.; Soulier, J.-L.; Sicsic, S.; Piarulli, U.; Reboud-Ravaux, M.; Ongeri, S. *ChemMedChem* **2010**, *5*, 1899−1906.
(41) Quere, L.; Wenger, T.; Schramm, H. J. *Biochem. Biophys. Res. Commun.* **1996**, *227*, 484−488.
(42) Breccia, P.; Boggetto, N.; Perez-Fernandez, R.; Gool, M. V.; Takahashi, M.; Rene, L.; Prados, P.; Badet, P.; Reboud-Ravaux, M.; Mendoza, J. D. *J. Med. Chem.* **2003**, *46*, 5196−5107.
(43) McGovern, S. L.; Caselli, E.; Grigorieff, N.; Shoichet, B. K. *J. Med. Chem.* **2002**, *45*, 1712−1722.
(44) McGovern, S. L.; Shoichet, B. K. *J. Med. Chem.* **2003**, *46*, 1478−1483.
(45) Ryan, A. J.; Gray, N. M.; Lowe, P. N.; Chung, C.-w. *J. Med. Chem.* **2003**, *46*, 3448−3451.
(46) Zutshi, R.; Franciskovich, J.; Shultz, M.; Schweitzer, B.; Bishop, P.; Wilson, M.; Chmielewski, J. *J. Am. Chem. Soc.* **1997**, *119*, 4841−4845.